Prognostic Value of the Optimal Measurement Location of On-site CT-derived Fractional Flow Reserve

Journal of Cardiology 80 (2022) 14–21

Contents lists available at ScienceDirect

Journal of Cardiology

journal homepage: www.elsevier.com/locate/jjcc

Original Article

Prognostic value of the optimal measurement location of on-site CT-derived fractional flow reserve

Yui O. Nozaki (MD) [a], Shinichiro Fujimoto (MD, PhD, FJCC) [a,*], Yuko O. Kawaguchi (MD, PhD) [a], Chihiro Aoshima (MD, PhD) [a], Yuki Kamo (MD, PhD) [a], Hideyuki Sato (MS, RT) [a,b], Hikaru Kudo (RT) [b], Kazuhisa Takamura (MD, PhD) [a], Ayako Kudo (MD) [a], Daigo Takahashi (MD) [a], Makoto Hiki (MD, PhD) [a], Tomotaka Dohi (MD, PhD, FJCC) [a], Nobuo Tomizawa (MD, PhD) [c], Kanako K. Kumamaru (MD, PhD) [c], Shigeki Aoki (MD, PhD) [c], Tohru Minamino (MD, PhD, FJCC) [a,d]

[a] Department of Cardiovascular Biology and Medicine, Juntendo University Graduate School of Medicine, Tokyo, Japan
[b] Department of Radiological Technology, Juntendo University Hospital, Tokyo, Japan
[c] Department of Radiology, Juntendo University Graduate School of Medicine, Tokyo, Japan
[d] Japan Agency for Medical Research and Development-Core Research for Evolutionary Medical Science and Technology (AMED-CREST), Japan Agency for Medical Research and Development, Tokyo, Japan

ARTICLE INFO

Article history:
Received 7 January 2022
Received in revised form 14 February 2022
Accepted 25 February 2022
Available online 29 March 2022

Keywords:
Coronary computed tomography angiography
Fractional flow reserve
Fluid structure interaction
Lesion-specific ischemia
Prognosis

ABSTRACT

Background: On-site computed tomography-derived fractional flow reserve (CT-FFR), using fluid structure interaction during multiple optimal diastolic phases, is of incremental diagnostic value. However, few studies have investigated prognosis, with the appropriate measurement location of CT-FFR, as a stand-alone modality. The aim of the present study was to assess the clinical impact on CT-FFR with an appropriate measurement.
Methods: A total of 370 consecutive patients (68 ± 10 years, 75% male) who underwent coronary CT angiography (CCTA), showing 50–90% stenosis in at least one major epicardial vessel, were retrospectively analyzed and followed up for a median 2.9 years. CT-FFR values were measured at three points: 1 to 2 cm distal to the target lesion ($CT\text{-}FFR_{1cm,\ 2cm}$) and the vessel terminus ($CT\text{-}FFR_{lowest}$), and a CT-FFR value ≤0.80 was considered to be abnormal. The endpoint was major adverse cardiovascular events (MACE), a composite of cardiac death, non-fatal myocardial infarction, and unplanned revascularization.
Results: The incidence of MACE was 6.8% (25/370 patients). The Kaplan-Meier survival analysis in negative $CT\text{-}FFR_{1/2cm}$ revealed no significant difference in MACE between negative and positive $CT\text{-}FFR_{lowest}$ [$p = 0.11/0.23$ (1/2 cm vs lowest)]. Among 221 patients who did not undergo planned revascularization within 90 days of CCTA, no significant differences were noted in the incidence of MACE between negative and positive $CT\text{-}FFR_{lowest}$ ($p = 0.11$). In contrast, the risk of MACE was significantly higher with positive $CT\text{-}FFR_{1/2cm}$ [$p = 0.0198/0.0002$ (1/2 cm)].
Conclusions: In terms of the prognosis of patients with moderate to severe stenosis on CCTA, CT-FFR measured 1 to 2 cm distal to the target lesion may be feasible for the safe deferral of unnecessary invasive coronary angiography. Moreover, $CT\text{-}FFR_{1/2cm}$ showed better risk stratification than $CT\text{-}FFR_{lowest}$ based on future adverse cardiac events.

Introduction

Computed tomography-derived fractional flow reserve (CT-FFR) provides anatomical and physiological assessments of coronary artery disease (CAD) and has demonstrated high diagnostic performance and a good correlation with invasive FFR for detecting flow-limiting stenosis [1–6].

One of the methods for on-site CT-FFR, calculates coronary flow and pressures by accounting for the shape, movement, cross-sectional area, and changes in the volume of the coronary artery using fluid structure interaction during multiple optimal diastolic phases of the cardiac cycle on 320-row area detector CT [7,8]. The next challenge facing CT-FFR is the identification of an ideal position for simple and singular CT-FFR evaluations of CAD. We previously demonstrated that CT-FFR

* Corresponding author at: Department of Cardiovascular Biology and Medicine, Juntendo University Graduate School of Medicine, 2-1-1 Hongo Bunkyo-ku, Tokyo 113-8421, Japan.
E-mail address: s-fujimo@tj8.so-net.ne.jp (S. Fujimoto).

https://doi.org/10.1016/j.jjcc.2022.02.019
0914-5087/

measured 1 to 2 cm distal to a target stenosis more strongly correlated with the result of invasive FFR than that measured at the vessel terminus [9]. However, the clinical utility and outcome data of optimal CT-FFR measurements have not yet been examined. Although previous studies reported short-to-intermediate clinical outcomes using FFR_{ct}, which derived from full 3D computational fluid dynamics [10–15], no previous study has investigated outcomes with an appropriate measurement location on FFR_{ct}, to our knowledge.

Therefore, the aim of the present study was to assess the prognostic impact of CT-FFR on patients with 50–90% stenosis on CCTA.

Patients and methods

Study design

This was a single-center, retrospective study. We recruited 413 consecutive patients with suspected CAD who underwent CCTA in a single-heartbeat scan with a phase window of 70% to 99% of the R-R interval, showing 50 to 90% stenosis in at least one major vessel with a segment of 1.8 mm or greater, between December 2015 and September 2019 after excluding known CAD [a history of myocardial infarction (MI), prior coronary revascularization, or the status of acute coronary syndrome]. Patients were also excluded from the analysis for the following reasons: inadequate CCTA image quality ($n = 3$), lost to follow up after less than 90 days ($n = 23$), small vessels (diagonal branch etc.) ($n = 14$), or unable to be analyzed for CT-FFR ($n = 3$). Therefore, the remaining 370 patients (606 vessels) were ultimately analyzed.

The study period was limited before any CT-derived FFR (FFR_{ct} HeartFlow Inc., Redwood City, CA, USA) was applied to clinical practice, and thus, all patients were followed up based on the clinical decisions of local physicians based on the CCTA result without any CT-derived FFR results.

The study was approved by the institutional medical ethics committee and complied with the Declarations of Helsinki. The need for informed consent was waived because of the retrospective study.

CCTA acquisition and interpretation

Detailed information is provided in Online File 1.

CT-FFR analysis and measurement

CT-FFR analysis was performed on a workstation (Vitrea version V7.2; Vital Images In, Minnetonka, MN, USA). The centerline and luminal contours of the three major coronary arteries were automatically selected, and manual adjustments were performed where necessary. After the procedure, CT-FFR was calculated using the analysis software (Canon Medial Systems Corporation, Otawara, Japan), which allows the computation of CT-FFR values at any selected points of the coronary tree. CT-FFR was calculated according to the fluid structure interaction, in consideration of changes in the shape, movement, cross-sectional area, and volume of the coronary artery using several optimal cardiac phases to acquire 70–99% of the cardiac phase [16,17]. Hierarchical Bayes & Markov-Chain Monte Carlo Methods were applied to determine conditions for the analysis. Furthermore, on-site analysis was performed by calculating 1D computational fluid dynamics. All procedures were conducted by a skilled analyst with >50 h of training experience with the software and who was blinded to the outcomes. The degree of coronary artery stenosis and the following three parameters were calculated by a consensus of three experienced cardiovascular imagers who were blinded to clinical data: the lowest CT-FFR value at the distal end of the target coronary vessel ($CT\text{-}FFR_{lowest}$), and the CT-FFR values 1 and 2 cm distal to the end of the stenotic lesion in the 50% to 90% range ($CT\text{-}FFR_{1cm,\ 2cm}$). These parameters were all computed locally on a regular workstation. The locations at which these parameters of CT-FFR are measured have already been described in a previous study [9]. Briefly, CT-FFR was measured 1, 2 cm distal to the target stenosis and at the terminus in a target vessel with 50% to 90% stenosis on CCTA, and a CT-FFR value ≤0.80 was considered to be abnormal. In each measurement of $CT\text{-}FFR_{1cm,\ 2cm,}$ and $_{lowest}$, the lowest CT-FFR value was registered when a patient had two- or three-vessel diseases.

Clinical endpoints

The primary endpoint was a composite of major cardiovascular adverse events (MACE) (cardiac death, non-fatal MI, and unplanned revascularization). Revascularization with either percutaneous coronary intervention or coronary artery bypass graft (CABG) was categorized as planned or unplanned. Decisions regarding revascularization were made at the discretion of the attending physician according to standard practices [18]. Planned revascularization was defined as that planned after the initial decision from within 90 days of CCTA. Unplanned revascularization was defined as any subsequent revascularization that was not scheduled in the immediate post-CCTA test period at a minimum of 90 days from CCTA. Cardiac death and MI were defined based on presently published guidelines. All deaths were considered to be cardiac in nature unless an undisputable non-cardiac cause was identified. MI was defined according to an expert consensus document [19].

There were two secondary endpoints: (a) a composite of all-cause death, non-fatal MI, and unplanned revascularization, and (b) a composite of cardiac/all-cause death and non-fatal MI (critical event).

The follow-up period began on the day of the CT scan and continued until the clinical end or end of study period, namely, December 31, 2020. All clinical events were obtained from medical records and/or telephone interviews until the end of the study period. All analyses were performed as time to the first endpoint event. The cumulative incidence of the combined endpoint was assessed in 2 or 3 groups of patients. Two groups were divided based on the positivity in CT-FFR for the three measurement points. Three groups were divided into group 1 (negative $CT\text{-}FFR_{lowest,}$), group 2 (negative $CT\text{-}FFR_{1/2cm}$ + positive $CT\text{-}FFR_{lowest}$), and group 3 (positive $CT\text{-}FFR_{1/2cm}$).

Statistical analysis

Descriptive statistics are shown as means and standard deviation for continuous variables and frequencies and percentages for categorical variables. Revascularization in CT-FFR measurements were compared using the chi-squared test. The diagnostic prediction for planned revascularization calculated with accuracy, sensitivity, specificity, positive predictive value (PPV), and negative predictive value (NPV) with 95% confidence intervals (CIs) and compared among each CT-FFR measurement. Comparisons of the cumulative incidence of the primary and secondary endpoints were conducted using the Kaplan-Meier method with the log-rank test. An analysis of the time to the first event was performed using Cox's proportional hazard regression models to estimate hazard ratios (HRs) with 95% CIs to assess the relationship of each index of CT-FFR. A 2-sided p-value <0.05 was considered to be indicative of significance. Statical analyses were performed using JMP pro 14.2 software (SAS institute INC., Cary, NC, USA).

Results

Study flow chart and characteristics

A flow chart of the present study is shown in Fig. 1. The final analysis was performed on 370 patients with 606 vessels, with a median follow up of 2.9 (range 1.0–3.9) years.

The mean age of patients (75.2% male) was 68 years ±10.1. Perpatients characteristics are summarized in Online Table 1. Approximately 45% (168/370) of patients had multi-vessel diseases on CCTA. Significant stenosis was found, and subsequent CT-FFR was performed more frequently on left anterior descending artery (48.9%, 297 vessels)

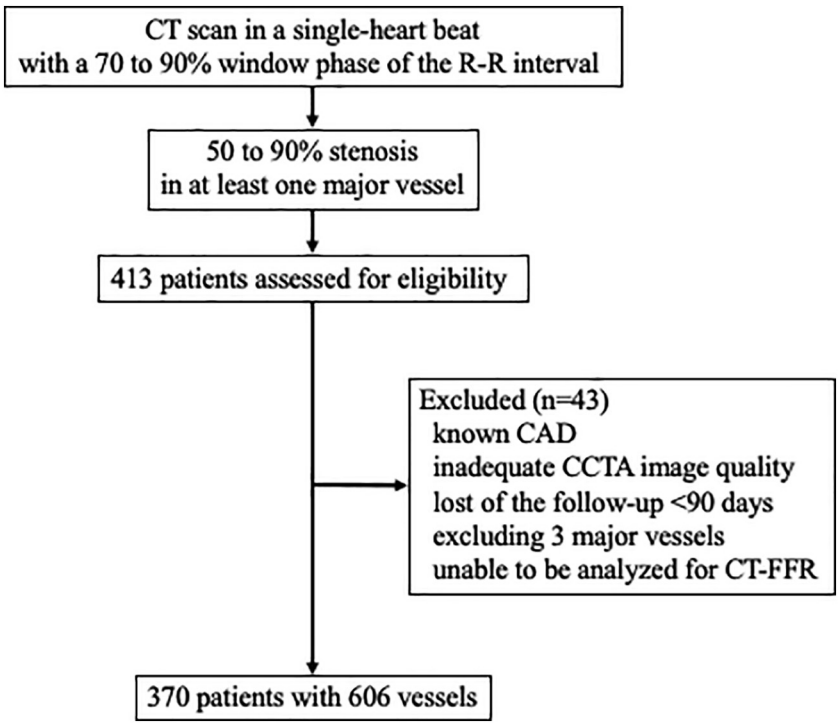

Fig. 1. Inclusion flow chart.
CAD, coronary artery disease; CCTA, coronary CT angiography; CT, computed tomography; CT-FFR, fractional flow reserve derived from coronary computed tomography angiography.

than on left circumflex artery, or right coronary artery. Mean per-patient CT-FFR$_{1cm,\ 2cm,}$ and $_{lowest}$ values were 0.82 ± 0.15, 0.80 ± 0.16, and 0.63 ± 0.20, respectively.

Planned revascularization was performed on 149 out of 370 patients (CABG; 22 cases). Most patients undergoing early revascularization had a CT-FFR$_{1/2cm}$ value ≤0.80, however, the ratio of early revascularization decreased in CT-FFR$_{lowest}$ [1 cm: 82.5% (113/137), 2 cm: 74.2% (121/163), lowest: 44.8% (147/328)]. A total of 136 (36.8%), 167 (45.1%), and 328 (88.6%) patients had a CT-FFR value of 0.80 or less at 1 cm and 2 cm distal to a target lesion and at vessel terminus, respectively, and 83.8% (114/136), 73.1% (122/167), and 45.4% (149/328) of these patients underwent planned revascularization. The per-patient sensitivity, specificity, PPV, NPV, and diagnostic accuracy of CT-FFR$_{1cm,\ 2cm,}$ and $_{lowest}$ to detect planned revascularization in clinical practice are shown in Table 1. The per-vessel diagnostic accuracy is shown in Online Table 2. The diagnostic accuracy was higher for CT-FFR$_{1cm,\ 2cm}$ than for CT-FFR$_{lowest}$.

Primary endpoints for all study patients

The incidence of adverse events was 8.4% (31 out of 370 patients), including 10 all-cause (including four cardiac deaths), 2 non-fatal MIs, and 20 unplanned revascularizations. MACE occurred in 6.8% (25 out of 370 patients). There was one duplicate case; one cardiac death occurred after unplanned revascularization. Online Fig. 1 shows the MACE rate in groups stratified by each CT-FFR value 0.05.

The Kaplan-Meier curve for MACE is shown in Fig. 2. In the three groups (group 1: negative CT-FFR$_{lowest}$, group 2: negative CT-FFR$_{1/2cm}$ + positive FFR$_{lowest}$, group 3: positive CT-FFR$_{1/2cm}$), significant differences were observed in both CT-FFR$_{1cm}$ and CT-FFR$_{2cm}$ in MACE for all [p = 0.0094 (CT-FFR$_{1cm}$), 0.0002 (CT-FFR$_{2cm}$)]. Significant differences were observed for group 1 vs group 3 [p = 0.0138 (CT-FFR$_{1cm}$), 0.0019 (CT-FFR$_{2cm}$)] and group 2 vs group 3 [p = 0.0289 (CT-FFR$_{1cm}$), 0.0008 (CT-FFR$_{2cm}$)], but not between groups 1 and 2 [p = 0.11 (CT-FFR$_{1cm}$), 0.23 (CT-FFR$_{2cm}$)]. The subgroup analysis was performed in patients with higher coronary artery calcium score (CACS) (Agatston score ≥ 400) (Online Fig. 2).

The results of Cox's regression analysis of the primary endpoint are summarized in Table 2. A univariable analysis for the primary endpoint identified multi-vessel disease and the lesion-specific CT-FFR value as significant factors [multi-vessel disease HR, 3.9 (p = 0.0037; 95%CI 1.56–9.79)], CT-FFR$_{1cm}$ HR, 3.0 [p = 0.0080 (1.33–6.79)], and CT-FFR$_{2cm}$ HR, 6.2 [p = 0.0094 (2.26–16.96)].

Table 1
Per-patient comparison among three measurements for CT-FFR to identify planned revascularization followed by the conventional strategy.

CT-FFR	Sensitivity (%) (95% CI)	Specificity (%) (95% CI)	PPV (%) (95% CI)	NPV (%) (95% CI)	Accuracy (%) (95% CI)
1 cm	75.5 (70.6–79.4)	90.0 (86.6–92.7)	83.8 (78.4–88.2)	84.2 (81.1–86.7)	84.1 (80.1–87.3)
2 cm	80.8 (75.6–85.2)	75.3 (70.5–79.4)	75.3 (70.5–79.4)	86.1 (82.3–89.2)	81.4 (77.1–84.9)
lowest	98.7 (95.7–99.6)	18.3 (16.2–18.9)	45.4 (44.1–45.9)	95.2 (84.7–98.7)	51.1 (48.7–51.9)

CT-FFR, fractional flow reserve derived from coronary computed tomography angiography PPV, positive predictive value; NPV, negative predictive value; CI, confidence intervals.

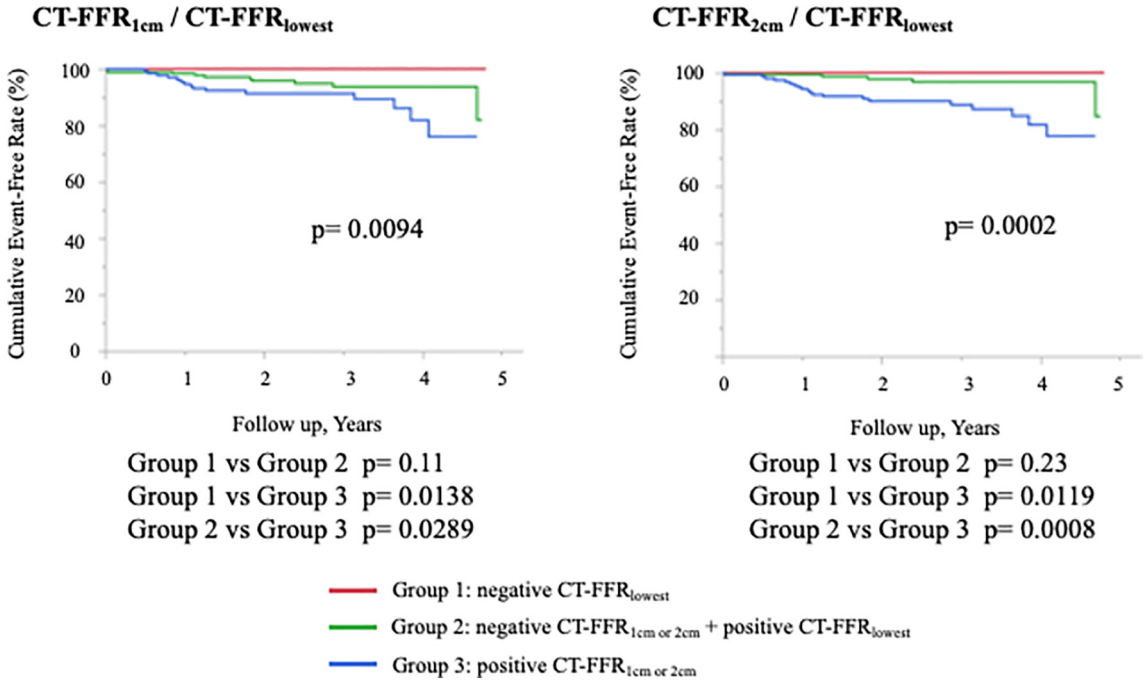

Fig. 2. Kaplan-Meier curve of the primary endpoint (major adverse cardiovascular events) for CT-FFR in all patients. Patient stratification according to negative / positive CT-FFR$_{1/2cm}$ and CT-FFR$_{lowest}$. The y-axis represents the cumulative event-free rate (the log-rank test *p*-value).
CT-FFR, fractional flow reserve derived from coronary computed tomography angiography.

Conventional risk factors, such as age, body mass index, and coronary risk factors, were not identified as significant factors in Cox's regression analysis.

Primary endpoints for patients without planned revascularization

A total of 221 patients did not undergo planned revascularization. Among these patients, significant differences were not observed in CT-FFR$_{lowest}$ in the incidence of MACE ($p = 0.11$). In contrast, the risk of MACE was significantly higher with positive CT-FFR$_{1cm}$ and CT-FFR$_{2cm}$ [$p = 0.0198$ (CT-FFR$_{1cm}$), 0.0002 (CT-FFR$_{2cm}$)] (Fig. 3). The subgroup analysis was also performed in patients with higher CACS (Online Fig. 3). The results of Cox's regression analysis are summarized in Table 2. A univariable analysis of this population also identified the same significant factors of multi-vessel disease and the lesion-specific CT-FFR value [multi-vessel disease HR, 3.9 ($p = 0.0468$; 95%CI 1.0–15.5), CT-FFR$_{1cm}$ HR, 4.5 ($p = 0.0036$; 1.1–18.0), and CT-FFR$_{2cm}$ HR, 8.8 ($p = 0.0021$; 2.2–35.4)].

Table 2
Univariate Cox's regression analysis of MACE.

	All patients $n = 370$			Patients without planned revascularization $n = 221$		
	HR	95% CI	*p*-value	HR	95% CI	*p*-value
Age	0.97	0.94–1.00	0.09	1.00	0.94–1.07	0.93
Sex (Male)	1.38	0.52–3.67	0.52	3.32	0.41–26.61	0.26
BMI	1.1	0.99–1.21	0.07	1.05	0.88–1.22	0.57
HTN	1.37	0.59–3.18	0.46	1.25	0.31–5.02	0.74
DM	1.17	0.54–2.58	0.69	2.5	0.62–9.98	0.20
DL	0.72	0.31–1.66	0.44	0.74	0.18–2.97	0.67
CACS Moderate CACS[a]	4.66	1.00–21.69	0.0498	2.94	0.30–28.53	0.35
Ref: low CACS High CACS[b]	4.27	0.97–18.84	0.06	3.09	0.36–26.51	0.30
Ref: low CACS Smoking	0.84	0.25–2.80	0.76	–	–	
CKD	1.13	0.42–3.02	0.80	0.52	0.06–4.17	0.50
71–90% stenosis[c] Ref: 50–70% stenosis	1.26	0.57–2.81	0.57	2.41	0.60–9.63	0.22
Multi-vessel disease	3.90	1.56–9.79	0.0037	3.86	1.56–9.79	0.0468
CT-FFR$_{1cm}$ ≤ 0.8	3.01	1.33–6.79	0.0080	4.50	1.12–18.03	0.0036
CT-FFR$_{2cm}$ ≤ 0.8	6.20	2.26–16.96	0.0004	8.83	2.20–35.40	0.0021

MACE, major adverse cardiac event; BMI, body mass index (kg/m^2); HTN, hypertension; DM, diabetes mellitus; DL, dyslipidemia; CACS, coronary artery calcium score; CKD, chronic kidney disease (eGFR≤60 ml/min/1.73m^2); CT-FFR, fractional flow reserve derived from coronary computed tomography angiography.
[a] Moderate CACS; Agatston score 100–399 as reference of low CACS (Agatston score < 100).
[b] High CACS; Agatston score ≥ 400 as reference of Agatston score < 100.
[c] ≥70% stenosis; maximum stenosis ≥70% at CCTA.

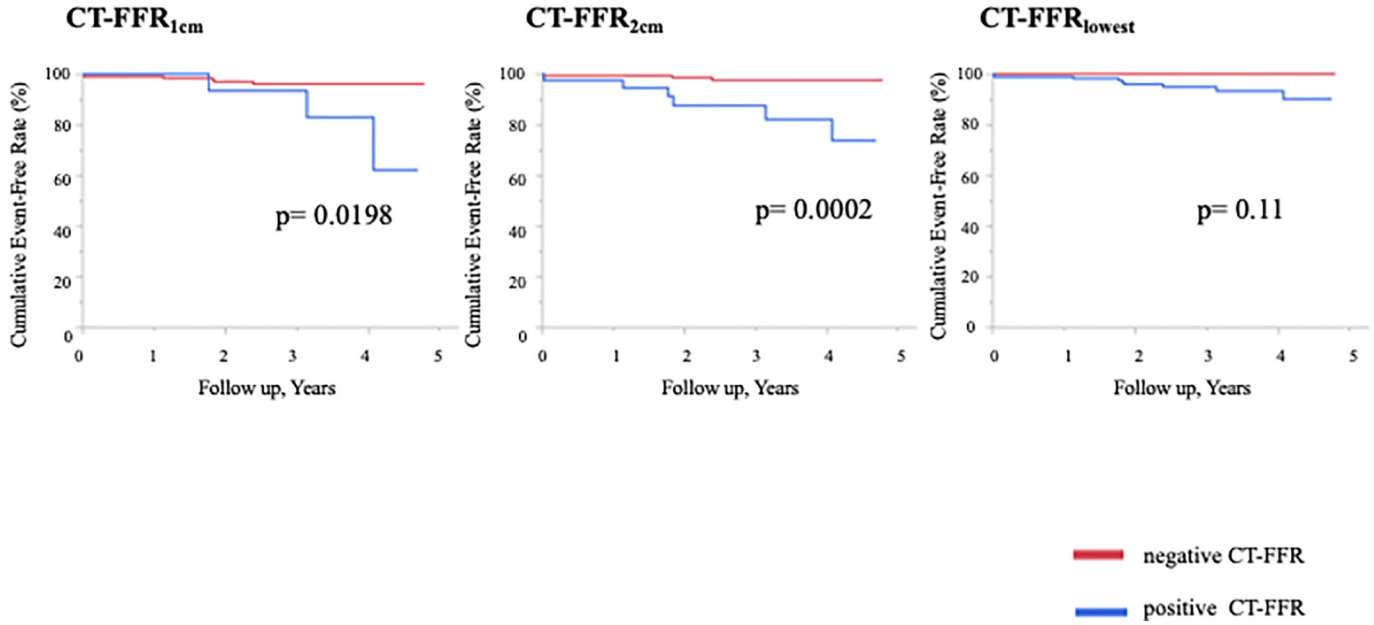

Fig. 3. Kaplan-Meier curve of the primary endpoint (MACE) for CT-FFR in patients without planned revascularization. Patient stratification according to negative or positive CT-FFR. MACE, major adverse cardiac event; CT-FFR, fractional flow reserve derived from coronary computed tomography angiography.

The analysis of a composite of all-cause death, non-fatal MI, and unplanned revascularization for all patients and excluded patients who underwent planned revascularization is summarized in Online File 2.

Secondary end points for all study patients and patients without planned revascularization

On the other hand, there were no differences in the rates of cardiac/all-cause death nor non-fatal MI (critical events) among the negative and positive groups in CT-$FFR_{1cm,\ 2cm,}$ and $_{lowest}$ in the entire cohort (Fig. 4a, b), as well as in the cohort excluding patients who underwent planned revascularization (Fig. 4c, d). In the univariable analysis of the critical events, no significant factor was identified, including multivessel or the lesion-specific CT-FFR value (Table 3).

Discussion

The present study was a CT-FFR-based analysis of 370 patients with suspected CAD who were clinically referred for CCTA and followed up for death, non-fatal MI, and unplanned revascularization for a median of 2.9 years.

In patients with 50 to 90% stenosis in at least one major vessel, the main results obtained were that: (1) CT-$FFR_{1/2cm}$ was a more consistent measurement with the conventional indication of planned revascularization than CT-FFR_{lowest}, when retrospectively analyzed; (2) among all patients, negative CT-$FFR_{1/2cm}$ deferred additional tests, including invasive coronary angiography (ICA) and revascularization, regardless of the results of CT-FFR_{lowest}; and (3) among patients who did not undergo early revascularization, CT-$FFR_{1/2cm}$ was a prominent measurement for the risk stratification on future cardiac events compared to CT-FFR_{lowest}.

The result of planned revascularization ratio in each CT-FFR value demonstrated that CT-$FFR_{1/2cm}$ was in close agreement with planned revascularization followed by the conventional management, compared to CT-FFR_{lowest}, which confirmed our previous study that concluded CT-$FFR_{1/2cm}$ had higher discrimination than CT-FFR_{lowest} against invasive FFR as a reference standard [9]. However, it currently remains unclear whether CT-$FFR_{1/2cm}$ is a prognostic measurement because we previously did not include outcomes.

Among the three groups classified by negative or positive CT-$FFR_{1,2cm}$ and CT-FFR_{lowest}, no significant difference was observed for MACE between patients with negative CT-FFR_{lowest} and those with negative CT-$FFR_{1/2cm}$ + positive CT-FFR_{lowest}. However, the only significant difference in MACE was found between the negative and positive CT-$FFR_{1/2cm}$ groups. This result implies that patients with negative CT-$FFR_{1/2cm}$ may safely defer ICA. In the present study, 58.2% (191/328) and 50.3% (165/328) of patients with positive CT-FFR_{lowest} were reclassified as negative with CT-FFR_{1cm} and $_{2cm}$, respectively, which was consistent with previous findings [14,20]. This result demonstrated that the deferral of unnecessary ICA and subsequent revascularization based on negative CT-$FFR_{1/2cm}$ was safe from the viewpoint of prognosis. Previous studies reported favorable short- to mid-term clinical outcomes with negative FFR_{ct} [10–15]. However, this is the first study to investigate the prognosis of patients using on-site CT-FFR, and the results obtained clearly showed a significant difference in prognosis between negative and positive of CT-$FFR_{1/2cm}$, but not CT-FFR_{lowest}.

Patients who did not undergo planned revascularization were also analyzed. This subgroup was a unique population that excluded the limitation of this retrospective study as much as possible because the whole population may be biased due to revascularization. Previous multicenter studies clarified the optimal prognosis of patients using CT-derived FFR, but included patients who underwent revascularization following CCTA and CT-derived FFR [10–13,15]. However, this subgroup in the present study was analyzed for the first time, in which the utility of CT-derived FFR and the following prognosis was examined for risk stratification on future cardiac events. The present study demonstrated that not CT-FFR_{lowest}, but CT-$FFR_{1/2cm}$ was a prominent measurement for future cardiac events, even when limited to patients with higher CACS. In contrast, no significant differences were observed in the rates of the critical events (deaths + non-fatal MI) among all measurements (CT-$FFR_{1cm,\ 2cm}$ and $_{lowest}$). One of the reasons was that it was primarily driven by a lower rate of non-fatal MI and death. The FAME-2 trial demonstrated the superiority of revascularization in positive invasive FFR over medical therapy, mainly due to a reduction in the need for urgent revascularization, but not the rate of death or MI [21,22]. Since prognostic research has generally been conducted on a per-patient level, the factors contributing to the critical events on a per-vessel level warrants

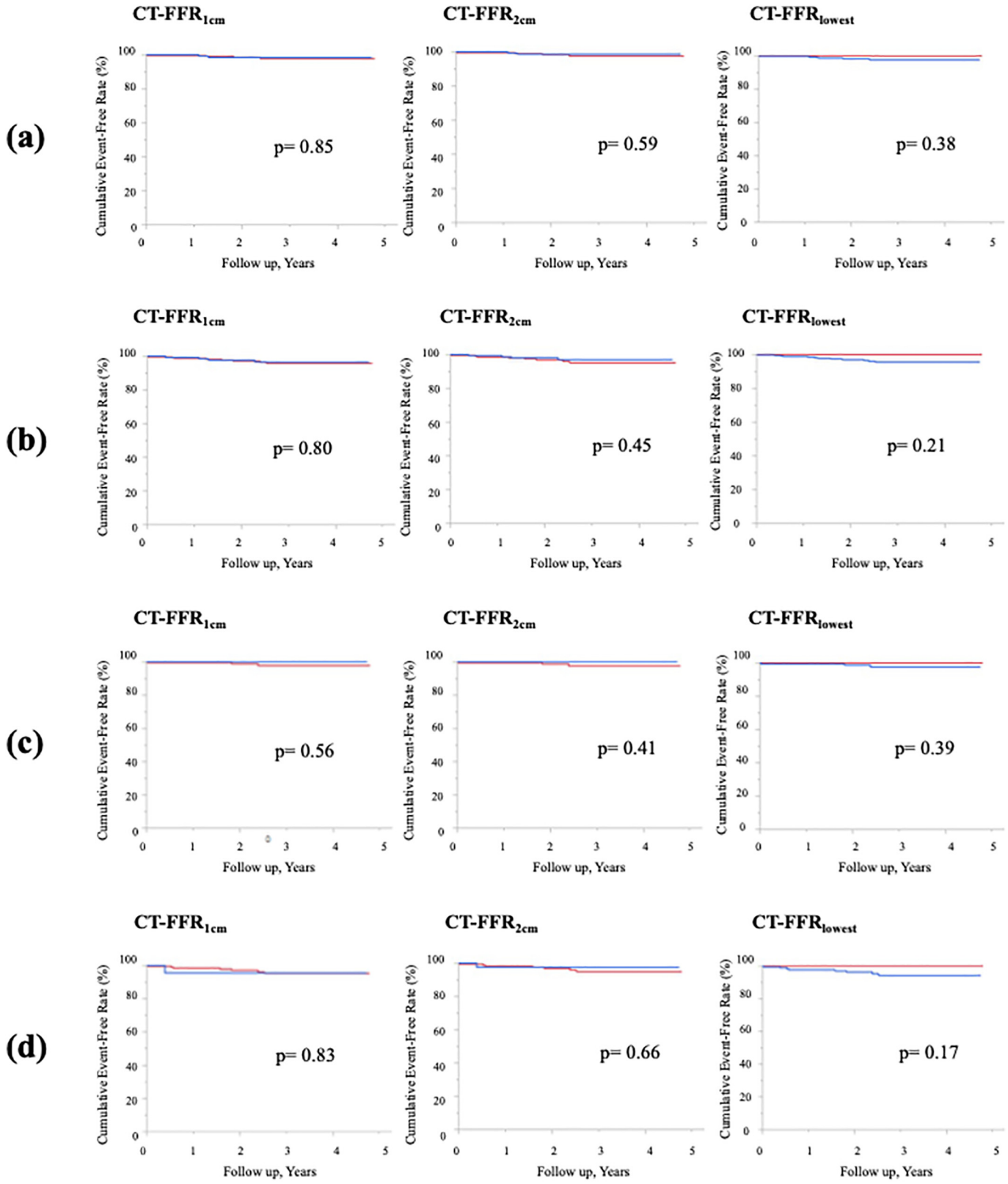

Fig. 4. Kaplan-Meier curve of the secondary endpoint [a composite of (a) cardiac death + non-fatal MI, and (b) all-cause death and non-fatal MI] for CT-FFR in all patients. Kaplan-Meier curve of the secondary endpoint [a composite of (c) cardiac death + non-fatal MI, and (d) all-cause death and non-fatal MI] for CT-FFR in patients who did not undergo planned revascularization. Patient stratification according to negative or positive CT-FFR.
MI, myocardial infarction; CT-FFR, fractional flow reserve derived from coronary computed tomography angiography.

Table 3
Univariate Cox's regression analysis of death and non-fatal MI.[a]

	Cardiac death + non-fatal MI			All-cause death + non-fatal MI		
	HR	95% CI	*p*-value	HR	95% CI	*p*-value
Age	1.00	0.93–1.08	0.91	1.02	0.96–1.11	0.53
Sex (Male)	0.32	0.07–1.61	0.19	0.66	0.16–2.76	0.58
BMI	0.95	0.75–1.19	0.67	0.83	0.66–1.20	0.09
HTN	1.25	0.23–6.82	0.79	1.02	0.24–4.29	0.97
DM	1.26	0.26–6.27	0.77	0.77	0.18–3.23	0.72
DL	0.34	0.07–1.70	0.19	0.64	0.15–2.70	0.55
CACS Moderate CACS[b]	2.65	0.27–25.46	0.40	1.76	0.32–9.64	0.52
Ref: low CACS High CACS[c]	1.07	0.10–12.84	0.96	0.59	0.08–4.22	0.60
Ref: low CACS Smoking	–	–	–	0.95	0.12–7.71	0.96
CKD	0.91	0.11–7.78	0.93	0.63	0.08–5.16	0.65
71–90% stenosis[d] Ref: 50–70% stenosis	0.79	0.16–3.91	0.77	1.11	0.35–3.50	0.86
Multi-vessel disease	3.86	1.56–9.79	0.0037	2.60	0.90–7.40	0.08
CT-FFR$_{1cm}$ ≤ 0.8	0.85	0.16–4.64	0.85	1.25	0.15–10.17	0.83
CT-FFR$_{2cm}$ ≤ 0.8	0.63	0.12–3.43	0.59	0.63	0.08–5.12	0.66

BMI, body mass index (kg/m^2); HTN, hypertension; DM, diabetes mellitus; DL, dyslipidemia; CACS, coronary artery calcium score; CKD, chronic kidney disease (eGFR≤60 ml/min/1.73m^2); CT-FFR, fractional flow reserve derived from coronary computed tomography angiography; MI, myocardial infarction.
[a] Moderate CACS, Agatston score 100–399 as reference of mild CACS (Agatston score < 100).
[b] High CACS, Agatston score ≥ 400 as reference of mild CACS (Agatston score < 100).
[c] 71–90% stenosis; maximum stenosis ≥70% at CCTA.
[d] 71-90% stenosis, maximum stenosis >70% at CCTA.

further investigation. Sudden death and MI were reportedly caused by the rupture of high-risk plaques, regardless of the severity of stenosis [23,24]. High-risk plaque features and endothelial wall shear stress on a target vessel may be predictors for a cardiac critical event [25–27]. Further studies are needed to assess the prognostic impact of these features on CCTA.

As described above, the CT-FFR-guided strategy was useful, associated with the utilization of fewer resources, and cost-effectiveness because of its on-site analysis. Beyond defining the clinical use and role of CT-FFR, our data provide meaningful insights into the potential prognostic value of CT-FFR in clinical practice. Importantly, negative CT-FFR$_{1/2cm}$ was associated with an excellent mid-term prognosis. The present study suggests that CT-FFR-guided decision-making has favorable mid-term outcomes, demonstrating the potential impact of adding non-invasively calculated CT-FFR to an anatomic strategy for the evaluation of CAD.

Limitations

There are a number of limitations that need to be addressed. This was a retrospective, single-center study on existing data, and thus, the influence of a potential selection bias cannot be excluded. The present study enrolled a relatively small number of patients. In addition, the number of events that occurred during the period was small, particularly following the division of patients into subgroups. A telephone survey to collect long-term follow-up data may have exposed patients to recall bias. Furthermore, the results of CCTA were summarized with a single classification based on the lowest CT-FFR even if multi-vessel diseases were examined. Therefore, the severity of multi-vessel disease may have been underestimated, particularly with the large burden of non-obstructive disease. Although we mentioned the importance of plaque morphology or wall shear stress in target vessels, other factors except CT-FFR were not included. In addition, the present study was based on a per-patient prognosis, and according to the results obtained, it was possible to reach a conclusion regarding whether a target vessel was not always the same as the culprit lesion. Moreover, CT-FFR analyses were not performed on stenoses with an estimated diameter of 30 to 50%, even if the stenosis showed diffuse coronary disease but under 50% stenosis on CCTA. Some stenoses that were not considered to be significant on CCTA may have been hemodynamically significant.

Conclusions

In patients with moderate to severe stenosis on CCTA, the conventional decision-making for planned revascularization was consistent with the results of CT-FFR$_{1\text{-}2cm}$. CT-FFR$_{1/2cm}$ is feasible for the safe deferral of unnecessary ICA from the viewpoint of clinical outcomes. Moreover, CT-FFR$_{1/2cm}$ showed more consistent risk stratification measurements than CT-FFR$_{lowest}$ based on future adverse cardiac events.

Supplementary data to this article can be found online at https://doi.org/10.1016/j.jjcc.2022.02.019.

Acknowledgments

We are indebted to Yosuke Kogure, RT, Hidekazu Inage, RT for technical assistance in this study.

Funding

This research was supported by Canon Medical Systems Corporation.

Declaration of competing interest

Dr. Fujimoto has a research agreement with Canon Medical Systems Corporation that is related to this study. All other authors report no conflicts of interest to the work.

References

[1] Koo BK, Erglis A, Doh JH, Daniels DV, Jegere S, Kim HS, et al. Diagnosis of ischemia-causing coronary stenoses by noninvasive fractional flow reserve computed from coronary computed tomographic angiograms. Results from the prospective multicenter DISCOVER-FLOW (diagnosis of ischemia-causing stenoses obtained via noninvasive fractional flow reserve) study. J Am Coll Cardiol 2011;58:1989–97.

[2] Solecki M, Kruk M, Demkow M, Schoepf UJ, Reynolds MA, Wardziak Ł, et al. What is the optimal anatomic location for coronary artery pressure measurement at CT-derived FFR? J Cardiovasc Comput Tomogr 2017;11:397–403.
[3] Min JK, Leipsic J, Pencina MJ, Berman DS, Koo B-K, Van Mieghem C, et al. Diagnostic accuracy of fractional flow reserve from anatomic CT angiography. JAMA 2012;308:1237.
[4] Coenen A, Lubbers MM, Kurata A, Kono A, Dedic A, Chelu RG, et al. Fractional flow reserve computed from noninvasive CT angiography data: diagnostic performance of an on-site clinician-operated computational fluid dynamics algorithm. Radiology 2015;274:674–83.
[5] Nørgaard BL, Leipsic J, Gaur S, Seneviratne S, Ko BS, Ito H, et al. Diagnostic performance of noninvasive fractional flow reserve derived from coronary computed tomography angiography in suspected coronary artery disease: the NXT trial (analysis of coronary blood flow using CT angiography: next steps). J Am Coll Cardiol 2014;63:1145–55.
[6] Tang CX, Liu CY, Lu MJ, Schoepf UJ, Tesche C, Bayer 2nd RR, et al. CT FFR for ischemia-specific CAD with a new computational fluid dynamics algorithm: a Chinese multicenter study. JACC Cardiovasc Imaging 2020;13:980–90.
[7] Fujimoto S, Kawasaki T, Kumamaru KK, Kawaguchi Y, Dohi T, Okonogi T, et al. Diagnostic performance of on-site computed CT-fractional flow reserve based on fluid structure interactions: comparison with invasive fractional flow reserve and instantaneous wave-free ratio. Eur Heart J Cardiovasc Imaging 2019;20:343–52.
[8] Ko BS, Cameron JD, Munnur RK, Wong DTL, Fujisawa Y, Sakaguchi T, et al. Noninvasive CT-derived FFR based on structural and fluid analysis. JACC Cardiovasc Imaging 2017;10:663–73.
[9] Nozaki YO, Fujimoto S, Aoshima C, Kamo Y, Kawaguchi YO, Takamura K, et al. Comparison of diagnostic performance in on-site based CT-derived fractional flow reserve measurements. Int J Cardiol Heart Vasc 2021;35:100815.
[10] Douglas PS, Pontone G, Hlatky MA, Patel MR, Norgaard BL, Byrne RA, et al. Clinical outcomes of fractional flow reserve by computed tomographic angiography-guided diagnostic strategies vs. usual care in patients with suspected coronary artery disease: the prospective longitudinal trial of FFR(CT): outcome and resource impacts study. Eur Heart J 2015;36:3359–67.
[11] Douglas PS, De Bruyne B, Pontone G, Patel MR, Norgaard BL, Byrne RA, et al. 1-year outcomes of FFRCT-guided care in patients with suspected coronary disease: the PLATFORM study. J Am Coll Cardiol 2016;68:435–45.
[12] Fairbairn TA, Nieman K, Akasaka T, Nørgaard BL, Berman DS, Raff G, et al. Real-world clinical utility and impact on clinical decision-making of coronary computed tomography angiography-derived fractional flow reserve: lessons from the ADVANCE registry. Eur Heart J 2018;39:3701–11.
[13] Patel MR, Nørgaard BL, Fairbairn TA, Nieman K, Akasaka T, Berman DS, et al. 1-year impact on medical practice and clinical outcomes of FFR(CT): the ADVANCE registry. JACC Cardiovasc Imaging 2020;13(1 Pt 1):97–105.
[14] Nørgaard BL, Terkelsen CJ, Mathiassen ON, Grove EL, Bøtker HE, Parner E, et al. Coronary CT angiographic and flow reserve-guided management of patients with stable ischemic heart disease. J Am Coll Cardiol 2018;72:2123–34.
[15] Ihdayhid AR, Norgaard BL, Gaur S, Leipsic J, Nerlekar N, Osawa K, et al. Prognostic value and risk continuum of noninvasive fractional flow reserve derived from coronary CT angiography. Radiology 2019;292:343–51.
[16] Hirohata K, Kano A, Goryu A, Ooga J, Hongo T, Higashi S, et al. A novel CT-FFR method for the coronary artery based on 4D-CT image analysis and structural and fluid analysis. Proc SPUE 2015:9412.
[17] Kato M, Hirohata K, Kano A, Higashi S, Goryu A, Hongo T, et al. Fast CT-FFR analysis method for the coronary artery based on 4D-CT image analysis and structural and fluid analysis. ASME 2015 Int Mech Eng Cong Expos 2015:V003T03A023.
[18] Naidu SS, Aronow HD, Box LC, Duffy PL, Kolansky DM, Kupfer JM, et al. SCAI expert consensus statement: 2016 best practices in the cardiac catheterization laboratory: (endorsed by the Cardiological Society of India, and Sociedad Latino Americana de Cardiologia Intervencionista; affirmation of value by the Canadian Association of Interventional Cardiology-Association Canadienne de Cardiologie d'Intervention). Catheter Cardiovasc Interv 2016;88:407–23.
[19] Thygesen K, Alpert JS, Jaffe AS, Simoons ML, Chaitman BR, White HD, et al. Third universal definition of myocardial infarction. J Am Coll Cardiol 2012;60:1581–98.
[20] Kueh SH, Mooney J, Ohana M, Kim U, Blanke P, Grover R, et al. Fractional flow reserve derived from coronary computed tomography angiography reclassification rate using value distal to lesion compared to lowest value. J Cardiovasc Comput Tomogr 2017;11:462–7.
[21] De Bruyne B, Fearon WF, Pijls NH, Barbato E, Tonino P, Piroth Z, et al. Fractional flow reserve-guided PCI for stable coronary artery disease. N Engl J Med 2014;371:1208–17.
[22] Xaplanteris P, Fournier S, Pijls NHJ, Fearon WF, Barbato E, Tonino PAL, et al. Five-year outcomes with PCI guided by fractional flow reserve. N Engl J Med 2018;379:250–9.
[23] Chang HJ, Lin FY, Lee SE, Andreini D, Bax J, Cademartiri F, et al. Coronary atherosclerotic precursors of acute coronary syndromes. J Am Coll Cardiol 2018;71:2511–22.
[24] Williams MC, Kwiecinski J, Doris M, McElhinney P, D'Souza MS, Cadet S, et al. Low-attenuation noncalcified plaque on coronary computed tomography angiography predicts myocardial infarction: results from the multicenter SCOT-HEART trial (Scottish Computed Tomography of the HEART). Circulation 2020;141:1452–62.
[25] Motoyama S, Sarai M, Harigaya H, Anno H, Inoue K, Hara T, et al. Computed tomographic angiography characteristics of atherosclerotic plaques subsequently resulting in acute coronary syndrome. J Am Coll Cardiol 2009;54:49–57.
[26] Lee JM, Choi G, Koo BK, Hwang D, Park J, Zhang J, et al. Identification of high-risk plaques destined to cause acute coronary syndrome using coronary computed tomographic angiography and computational fluid dynamics. JACC Cardiovasc Imaging 2019;12:1032–43.
[27] Ferencik M, Mayrhofer T, Bittner DO, Emami H, Puchner SB, Lu MT, et al. Use of high-risk coronary atherosclerotic plaque detection for risk stratification of patients with stable chest pain: a secondary analysis of the PROMISE randomized clinical trial. JAMA Cardiol 2018;3:144–52.